



Published in final edited form as:

Ann Biomed Eng. 2010 November ; 38(11): 3280–3294. doi:10.1007/s10439-010-0129-9.

Design and Validation of a Novel Splashing Bioreactor System for Use in Mitral Valve Organ Culture

Janet E. Barzilla, Ph.D¹, Anna S. McKenney, BS², Ashley E. Cowan, BS³, Christopher A. Durst, BS¹, and K. Jane Grande-Allen, Ph.D.¹

¹Dept of Bioengineering, MS-142; Rice University; PO Box 1892; Houston, TX 77251-1892

²Dept of Biomedical Engineering, Rensselaer Polytechnic Institute; Troy, NY 12180

³Dept of Biological Sciences, Murray State University; Murray, KY 42071-3361

Abstract

Previous research in our lab suggested that heart valve tissues cultured without mechanical stimulation do not retain their *in vivo* microstructure, i.e., cell density decreased within the deep tissue layers and increased at the periphery. In this study, a splashing rotating bioreactor was designed to apply mechanical stimulation to a mitral valve leaflet segment. Porcine valve segments (n=9–10 per group) were cultured in the bioreactor for two weeks (dynamic culture); negative controls were cultured without mechanical stimulation (static culture), and baseline controls were fresh uncultured samples. Overall changes in cellularity and ECM structure were assessed by H&E and Movat pentachrome stains. Tissues were also immunostained for multiple extracellular matrix (ECM) components and turnover mediators. After two weeks of culture, proliferating cells were distributed throughout the tissue in segments cultured in the bioreactor, in contrast to segments cultured without mechanical stimulation. Most ECM components, especially collagen types I and III, better maintained normal expression patterns and magnitudes (as found in baseline controls) over two weeks of dynamic organ culture compared to static culture. Lack of mechanical stimulation changed several aspects of the tissue microstructure, including the cell distribution and ECM locations. In conclusion, mechanical stimulation by the bioreactor maintained tissue integrity, which will enable future *in vitro* investigation of mitral valve remodeling.

Keywords

Extracellular matrix; collagen; proteoglycans; matrix metalloproteinases; lysyl oxidase; prolyl-4-hydroxylase; heat shock protein 47

INTRODUCTION

The successful creation of an *in vitro* experimental model of the mitral valve would provide a powerful tool for investigating the underlying mechanisms behind and possible treatments

for mitral valve disease. Although animal models have been used with great success in studying many forms of cardiovascular disease, these surgeries are invasive and costly. Additionally, a large number of animals would be required to study multiple early timepoints. Alternatives to surgical methods, such as molecular imaging to monitor valve remodeling, are being explored.¹⁴ Cell studies offer a less expensive alternative to animal studies; many recent studies of valvular biology and remodeling have employed cultures of valvular cells maintained in monolayers.^{35, 37, 40} This widely accepted protocol, however, does not allow investigators to investigate the basis for changes to the layered structure of the native valve, which can be greatly altered in valve disease.¹¹ Additionally, a monolayer culture imposes a drastic change in environmental stimuli for the cells, and thus may not accurately elicit the *in vivo* response.

To avoid the shortcomings of animal and cell models, we have chosen to investigate organ cultures, which maintain the valvular cells within the native physical structure of the tissue. Ideally, the organ cultures would be grown in conditions engineered to mimic the native environment. Organ cultures have successfully been established for a variety of tissues, including vascular intima,²⁵ canine leptomeninges,²⁹ mouse gallbladder epithelium,³⁶ brain hippocampal slices,³¹ and human lacrimal gland tissue.¹³ In human and mammalian heart valve tissues, short-term (6 day) organ cultures have been used to investigate wound healing responses.^{19–21}

Heart valve tissues are particularly appropriate for organ culture research because the cells within adult valves are nourished primarily through diffusive transport of oxygen and nutrients (as opposed to through vascularization⁴). It was therefore believed that designing a valvular organ culture system might be much simpler than designing systems for more complicated fully vascularized tissues. Previous work in our laboratory used a simple static system for organ culture (after Lester et al.^{19–21}) to demonstrate that the cells within the cultured valve tissues remained alive during long term culture periods (up to 7 weeks).¹ The aforementioned work also suggested, however, that static culture techniques alone did not maintain cell location. Fewer endothelial cells were noted on the cultured tissue. Although valvular interstitial cells were still present and viable after seven weeks, fewer cells were located deep within the tissue, suggesting migration of these cells to the periphery to obtain nutrients.¹

Since heart valves are continuously exposed *in vivo* to a variety of mechanical stresses from both myocardial motion and blood flow, it was further supposed that an *in vitro* system incorporating similar mechanical forces could maintain the valve structure. A number of bioreactor designs including flow loops,^{12, 15} cyclic pressure,^{28, 42} and cyclic flexure^{5–8, 26} systems are available for organ culture and tissue engineering applications. Many of these designs have specialized in the culture of semilunar (aortic and pulmonary) valves for a short period of time (approximately 48 hours). Although these bioreactor systems have been successful for their intended function, the present study was focused on the culture of atrioventricular (mitral and tricuspid) valve leaflets and their associated chordae tendinae. The present study was also designed for a longer timeframe (approximately 2 weeks).

To that end, a bioreactor was designed to provide cyclic, dynamic mechanical stimulation to an organ culture via sub-physiological fluid movement against the valve surfaces. These data were compared to porcine mitral and tricuspid valves cultured without mechanical stimulation to qualify valve remodeling over a period of several weeks. We hypothesized that the perfusion and gentle stretch provided by the dynamic un-quantified mechanical environment of the splashing bioreactor would be sufficient to maintain tissue structure and prevent cell migration. The successful validation of this system will allow future use of this bioreactor in both organ culture and tissue engineering applications.

METHODS

Pilot Long Term Static Culture Study

To determine the phenotypic effects of organ culturing without mechanical stimulation on heart valve tissue, organ cultures were established²⁰ for periods of time ranging from 0 to 8 weeks. Porcine tricuspid valves were used to prepare the valvular organ cultures in this study; porcine valves are widely used and accepted as anatomic^{18, 32} and biological models³⁷ for human valves. Valves (n=5) were obtained from a commercial abattoir, and the tricuspid valves were dissected from the hearts within 24 hours of removal from the body.

After removal of chordae tendinae and cardiac muscle tissue, the valve leaflets were dissected into 100 mm² blocks, yielding 5–10 blocks per individual valve. At each stage of culture establishment, care was taken to prevent physical disruption of the endothelial tissue layers. The organ culture blocks were then transferred to a sterile flow hood, gently rinsed in sterile phosphate-buffered saline (PBS), and placed into individual wells of 24-well tissue culture plates containing Medium 199 with modified HEPES buffer (Sigma, St. Louis, MO, USA) supplemented with 15% fetal bovine serum, 100 U/ml penicillin, 100 µg/ml streptomycin, and 0.25 µg/ml amphotericin B (all reagents from Invitrogen, Carlsbad, CA, USA). The organ cultures were maintained in a humidified incubator at 37°C with 5% CO₂ for up to 8 weeks. Culture medium was changed every 2 to 3 days. The resulting organ cultured blocks were removed before and after establishment of culture, and subsequently at weekly intervals for analysis.

At the specified time points, tissue blocks were removed from culture, fixed in Histochoice™ (Amresco, Solon, OH, USA), and embedded in paraffin. Tissue sections were stained with H&E and Movat pentachrome to identify the cell nuclei and extracellular matrix (ECM) components. Changes in the location of endothelial cells and in collagen synthesis were evaluated immunohistochemically using antibodies against von Willebrand Factor (vWF, Sigma) and the enzyme prolyl-4 hydroxylase (P4H, Chemicon, Temecula, CA, USA), respectively. The sample was first rehydrated using graded dilutions of Flex (Richard-Allen Scientific, Kalamazoo, MI). Antigen decloaking was performed using a citrate buffer, and the sample was exposed to a 10% solution of goat serum at room temperature for 1 hour to limit indiscriminate binding of the secondary antibody. After removing the goat serum, the appropriate primary antibody was applied and incubated at 37°C for 1 hour. Negative controls for each sample were exposed to the secondary antibody only. The primary antibody was then removed and the sample exposed to the biotinylated secondary goat anti-mouse antibody (Jackson ImmunoResearch, West Grove, PA) at room

temperature for 1 hour. The samples were then exposed to an avidin-biotin complex for 30 minutes and tagged using a 3,3'-diaminobenzidine kit for 10 minutes (both from Vector Labs, Burlingame, CA). All samples were counterstained with hematoxylin to localize cells within the tissue.

Bioreactor Design

The bioreactor chamber design consisted of 3 polycarbonate segments (McMaster-Carr, Chicago, IL), each 2" in diameter (Figure 1A). The segments were clamped together via four 4" long, 1/4"-28 partially threaded screws and nuts spaced 90° around the circumference of the bioreactor. The two ends of each segment each had 3 1/16" neoprene washers (McMaster-Carr) mounted using cyanoacrylate glue. The washers were wrapped with Teflon® tape upon chamber construction to prevent leaks. The main body of segment A was 1.5" tall and had a 1/2" hole in the center to accommodate fluid flow. The top of A was 1" tall and threaded to fit the vented filter cap from a 25 cm² tissue culture flask (BD Biosciences, San Jose, CA) in order to allow gas exchange in the bioreactor. Segment B was 5/8" tall and had a 1/2" hole in the center. Polyester mesh squares (Sefar America Inc, Depew, NY) approximately 0.5×1 mm were glued between the neoprene washers to provide a mounting location for the mitral valve. Segment C was 1.25" tall, and a 1/2" hole was cut through the top 1" for fluid flow. The bottom 1/4" of the segment was solid.

Repeatable fluid motion was provided by rotating the bioreactor chambers using a Labnet Mini LabRoller™ (ISC Bioexpress, Kaysville, UT). This rotator fit two bioreactors on a pallet, secured with two 3/16" cable ties (Figure 1B). The rotator, which was selected based on its small size and incubator compatibility, had only one available speed setting, rotating a full 360° at an approximate speed of 0.33 revolutions/second. This motion caused the media to splash across both valve surfaces, imparting a combination of normal and shear force to the valve; compression force from *in vivo* coaptation of the valve leaflet free edges would be absent (Figure 2). Based on previously published values of heart rate and tissue deformation in normal *in vivo* animal models^{16, 30}, it was assumed that tissue velocities and developed shear stresses in the bioreactor would be sub-physiological. A volume of 4.5 mL of culture medium was used to fill the chamber; although this volume of media only partially bathed the tissue when the chamber was not rotating, this volume allowed greater forces to be imparted onto the valve surface than would have been possible if the chamber had been completely filled.

Maximum tensile strains in the leaflet and the chordae were estimated separately due to the differences in the ECM structure of the two tissue types. Stress was first calculated from the normal force of the fluid on the submerged tissue, as given by the specific weight of the fluid and the tissue geometry. Strain was then calculated using the pre-transition stiffness of the tissue, which was estimated to be 5 times greater for chordae than leaflet^{17, 33}. As a result, the maximum tensile strain for leaflet (0.65%) was 5 times that of chordae (0.13%).

Maximum bending strains within regions of local curvature were estimated for both the leaflet and chordae by the ratio of one-half leaflet thickness to radius of curvature. This calculation was independent of material or geometry and was therefore applicable to both valve portions. Leaflet thickness was assumed to be 1 mm. Radius of curvature was

calculated from the chord length and arc length of the locally curved regions. To determine these lengths, it was assumed that the leaflet segment was straight across either one-half, two-thirds, three-fourths, or four-fifths of the annular to chordal attachment distance and the remainder of the leaflet segment was curved. These geometric conditions were estimated to generate maximal bending strains ranging from 4%, when the whole leaflet-chordal segment was bent in one smooth arc, to 25% when only one-fifth of the entire leaflet-chordal segment length was bent (Figure 2).

Additionally, a basic computational model was used to investigate the shear forces and fluid velocities imparted to the tissue by this system. ANSYS Workbench (ANSYS Inc, Canonsburg, PA) was used to run a computational fluid dynamics model of fluid flow across an idealized leaflet using the CFX code. Inlet flow rate (2.97 mL/s) was chosen from the fluid volume and rotation speed of the system. The flow was modeled as an inlet flow from the bottom surface of the lumen towards the top at four points through half of a system rotation (0°, 45°, 90°, 135° rotation). Calculations were performed using a shear stress transport model, which improves accuracy in the boundary region thereby increasing accuracy of wall shear stress calculations. This method employs a $k-\omega$ model at the wall and then blends it with a $k-\epsilon$ model.²⁴ Tissue wall shear stress was visualized on all surfaces of the leaflet, and the shear on the surface of the leaflet was determined by using a contour plot (Figure 3). Shear stress was observed to be consistent over the bulk of the leaflet surface and was observed to be 0.010–0.020 Pa at all orientations. Additionally, fluid velocities were investigated at the center plane of the culture chamber and visualized with a vector field (Figure 4), showing turbulence around the leaflet free edge.

Developing a bioreactor system that could be sterilized prior to assembly, and assembled and run in a sterile manner, was a major consideration during the design process. Prior to attachment of the valve segment in the bioreactor, the bioreactor was disassembled and the individual segments washed using a 1:128 dilution of CiDecon (Decon Labs, King of Prussia, PA) disinfectant. The segments were then sprayed with a 70% ethanol solution, with special attention paid to the inside surfaces, and exposed to ultraviolet light in a sterile biological hood for 30 minutes-1 hour. The bioreactor pieces remained in the sterile hood until assembly. Sterility testing of the bioreactor was performed by allowing media to remain in the stationary chamber for one week. Initial tests were performed without valve tissue, and later tests included a mitral valve segment mounted in the bioreactor chamber. When the media was changed, a sample of the old media was placed into a 6-well plate and returned to the incubator. A sample of the fluid was also applied to an agar plate and allowed to incubate for 3 days. Additionally, media was spot-checked for contamination during test runs with the valves by drawing media samples, incubating the media in a 6-well plate for 2–3 days, and examining the media using an inverted microscope.

Design Validation

Porcine mitral valves (Fisher Ham & Meat, Houston, TX) from animals approximately six months in age were used to validate the ability of the designed bioreactor to maintain the normal condition of the valve microstructure and cell distribution. Valves were dissected from the heart within 6–10 hours post mortem and rinsed in sterile PBS containing 5%

antibiotic/antimycotic solution (Mediatech Inc, Herndon, VA) to remove bacteria. Two 5 mm wide radial segments (one surrounding each strut chordae, Figure 5A) were then removed from the anterior leaflets (n=19 total). When preparing the tissue segments, the entire length of the leaflet (annulus to free edge) and strut chordae were used. Due to the similarity in the age of the animals from which the hearts were harvested, valve tissue segment sizes were generally consistent.

The first segment from each valve was cultured, under either static or dynamic conditions, for two weeks. Static cultures (negative control, n=10) were placed in a T-25 tissue culture flask. As with the pilot study, static cultures were not subjected to any mechanical stimulation. Dynamic cultures (n=9) were mounted in the bioreactor (Figure 5B, 5C); anchoring on both ends of the tissue was fixed, and did not contract as it would in the *in vivo* system. The valve segment was carefully mounted within the bioreactor in such a way that it was kept slack in order to model diastole, with the assumption that tension on the tissue culture during systole would be lower than on the *in vivo* tissue due to the lower *in vitro* fluid speed and lack of mechanical stimulation from the ventricular wall. In both test cases, the tissue was bathed in organ culture media (DMEM/Ham's F12, Mediatech Inc; 10% bovine growth serum, HyClone Waltham, MA; 1% HEPES buffer, Mediatech Inc) containing 5% antibiotic/antimycotic solution for the first 24 hours after dissection, after which it was replaced by media with 1% antibiotic/antimycotic solution. The second segment from each valve was designated a baseline control sample. All tissues were fixed in Histochoice™ after two weeks (cultured samples) or immediately after dissection (baseline control samples). After fixation, all tissue samples were dehydrated to xylene, paraffin embedded, sectioned into 5 µm slices, and mounted on slides.

As in the pilot study, samples in the validation study were stained with H&E and Movat pentachrome. Immunohistochemical staining was employed to localize the proteoglycans (PGs) versican (VC, Seikagaku, Associates of Cape Cod, East Falmouth, MA), decorin (DCN), and biglycan (BGL), as well as collagen types 1 and 3 (COLL1/COLL3), within the valve layers. Unless otherwise indicated, antibodies were generously provided by Larry Fisher, Ph.D. of NIH.⁹ In addition to these ECM components, the ECM synthesis mediators P4H (Millipore, Billerica, MA), lysyl oxidase (LOX, Imgenex, San Diego, CA), and heat shock protein 47 (HSP47, Abcam, Cambridge, MA) were also localized. HSP47 is a molecular chaperone associated with collagen synthesis, while LOX is involved in collagen and elastin cross-linking. Immunohistochemical staining for matrix metalloproteinases (MMPs) 1, 2, 9 (all from Assay Designs, Ann Arbor, MI), and 13 (Millipore) identified sites of enzymatic matrix degradation. Staining for tissue inhibitor of matrix metalloproteinase 1 (TIMP-1, Assay Designs) stain was also performed. An antibody sensitive to proliferating cell nuclear antigen (PCNA, Abcam) determined the location of proliferating cells within the tissue. The immunohistochemical method for PGs was identical to that of the P4H method described above, except for sample pretreatment with Chondroitinase ABC (Seikagaku, Tokyo, Japan) in lieu of antigen decloaking to expose the core protein binding site. No antigen retrieval step was required for the COLL1, COLL3, or MMP13 primary antibodies. Sections were then treated with biotinylated secondary antibodies derived from goat (anti-

rabbit or anti-mouse as appropriate, Jackson ImmunoResearch) prior to chromogenic staining.

All stained samples were imaged using a Microtek ArtixScan 4000tf slide scanner (Microtek International, Carson, CA). Images were then blinded and graded for staining intensity on a scale of 0 to 4: 0 indicated no stain; 1 indicated weak stain in <50% of the area of interest; 2 indicated weak stain in >50% or strong stain in <10%; 3 indicated strong stain in <50%; and 4 indicated strong stain in >50%. This semi-quantitative method has been used previously in our lab with a variability of <15%¹¹. In order to determine the effect of the mechanical stimulation throughout the tissue, staining intensities were assessed in all three valve leaflet layers: the elastin-rich atrialis, located at the atrial surface; the middle spongiosa layer, comprised of PGs and glycosaminoglycans (GAGs); and the collagenous fibrosa, located near the ventricular surface. Staining intensity was also measured in the strut chordae. Co-localization of the different ECM components and turnover mediators within the valve layers was performed via comparison of the immunohistochemically stained samples to the Movat stained samples. PCNA and H&E stained samples were examined qualitatively to assess changes in cellular density within the different valve layers.

Statistical Analysis

Since each anterior valve leaflet had two strut chordae (Figure 5A), each valve yielded two samples for testing. For each valve obtained during the validation study, one segment was designated a baseline control, and the second segment was cultured for two weeks in either the no mechanical stimulation (static) or cyclic mechanical stimulation (dynamic) condition; therefore, each test group had its own matched control. In every valve layer, staining intensity of each ECM component and turnover mediator of the cultured segment was normalized to that of the baseline control segment. A staining intensity within 20% of the baseline (normalized values of 1.0 ± 0.2) was considered to be maintenance of the component during the treatment period. Normalized staining intensities of the dynamic organ culture was compared to those of the static controls using a Student's t-test, with statistical significance defined as $p < 0.05$.

RESULTS

Pilot Long Term Static Culture Study

Several general trends were identified in the Movat stained atrioventricular valve samples cultured under static conditions over a period of several weeks. First, collagen became more diffusely distributed in all samples. Towards the end of the culture period, collagen either dominated the cross section or shared dominance with elastin (Figure 6A). The alcian blue stain marking the initially distinct PG layer became less well defined, then developed to a diffuse bluish haze within the collagen, and was virtually undetectable in the final week of the cultures (Figure 6B). Finally, elastin content increased in some samples, although the final distribution of the elastin varied greatly between valve samples (Figure 6C).

All tissue blocks taken at initial culture had an even distribution of cells on the interior, and a thin layer of endothelial cells on the outer surface (Figure 7). Care was taken during tissue

sectioning to limit damage to the endothelium, and staining performed prior to organ culture indicated that this layer was intact. In future studies, scanning electron microscopy could also be performed to confirm tissue integrity. In the first of three identified cell distribution patterns in the static cultures (Figure 8), a *clumping pattern* was observed, in which cells became more abundant in certain areas of the valve, often less dense regions containing PGs, and less abundant in the more dense collagen-rich regions. Next, a *depletory effect* was seen, in which few cells could be detected. Finally, there was an *accumulation of cells* on the surface of many organ cultures. This accumulation, which was especially pronounced in the first two weeks of culture, was located mainly on the ventricular surface of the valve and in areas containing sharp protrusions or indentations that acutely and locally disrupted the endothelial layer or well organized valve microstructure.

Cells staining for P4H were initially evenly distributed throughout the interior of the valve, but by the conclusion of culture, strong marker expression in the leaflet interior coincided with the accumulations of collagen shown in the Movat's pentachrome stain (data not shown). P4H also showed strong expression in the exterior cell accumulations. The results of the pilot study were used as a basis of comparison for the bioreactor validation studies.

Validation of Bioreactor Effectiveness

After the bioreactor was designed and built, it was tested to verify that it could maintain a sterile environment and that the mechanical stimulation would maintain ECM structure and cell viability. Sterility tests showed that the environment within the bioreactor remained free from contamination during the two week test period (data not shown).

The static culture results regarding the distribution of cells and the valvular layered structure corroborated those of the pilot study. PCNA immunostaining indicated that, without mechanical stimulation, fewer proliferating cells were located deep within the tissue, although proliferating cells were found near the tissue surface. H&E staining showed the same trend (data not shown). After two weeks of static culture, the layered structure of the valve was also compromised. Although the Movat image showed maintenance of the atrialis, the fibrosa and spongiosa became less defined, with an increase in collagen content in the normally PG-rich free edge spongiosa.

The bioreactor appeared to counteract these static culture trends; after two weeks of culture, cell concentrations in the middle and periphery appeared comparable to those in control tissue, as indicated by both H&E and PCNA staining. Positive immunostaining for PCNA (Figure 9) also suggested that these cells retained their ability to proliferate during the culture period. Additionally, tissue samples cultured in the bioreactor displayed a similar ECM structure to that of the control samples; the collagenous fibrosa and elastin-rich atrialis layers of the leaflet center were clearly delineated in the Movat images (Figure 9). The proteoglycans in the spongiosa of the free edge were also maintained (data not shown).

The use of matched baseline controls for both the static and dynamic culture groups allowed the staining intensities of the ECM components and the turnover mediators to be normalized for comparison of differences after two weeks of culture. A normalized value of 1 indicated that there was no change in the component after culture, while a value <1 indicated reduced

expression and a value >1 indicated greater expression. Overall, the splashing bioreactor was successful at maintaining most tested ECM components and turnover mediators (Table 1) as shown by maintenance of expression levels within 20% of baseline (normalized staining intensity of 1.0 ± 0.2). As shown in Figures 10–11, static culture generally reduced expression of these factors relative to baseline controls, while dynamic culture resulted in more clustering of normalized expression values around 1.0. In fact, more normalized values were within 10% of baseline for dynamic culture (28 out of 52 factors) than they were with static culture (22 out of 52 factors). The most distinctive results for each layer are noted below.

In the chordae, dynamic stimulation encouraged negligible changes in component expression when compared to static culture conditions (Figure 11A). Normal chordae consist of a collagen core surrounded by an elastin sheath. In the test samples, COL1 content was reduced in the static culture samples and maintained in the dynamic culture samples (0.65 ± 0.21 static vs. 1.1 ± 0.27 dynamic, $p<0.01$). Conversely, COL3 expression was elevated in the static samples and maintained in the dynamic samples (1.5 ± 0.82 static vs. 1.1 ± 0.14 dynamic). While VC expression (which was quite low in static culture samples) tended to improve with dynamic stimulation (0.53 ± 0.14 static vs. 0.87 ± 0.54 dynamic), DCN expression remained constant between the three groups (control, static, and dynamic). Expression of MMP1, MMP2, and TIMP1 between the three culture groups was also approximately equal. HSP47, MMP9, and MMP13 results were too varied to be conclusive. Dynamic culture caused expression of P4H, LOX, and BGN that was higher than the maintenance range (1.25 ± 0.42 , 1.29 ± 0.46 , and 1.39 ± 0.41 , respectively); in static culture conditions P4H and BGN were maintained (1.15 ± 0.46 and 0.92 ± 0.32 respectively) but LOX was reduced (0.69 ± 0.50).

The fibrosa of the normal mitral valve is also mostly comprised of COL1 and COL3. Normalized COL1 expression was approximately 1.0 for both the static and dynamic cases (0.94 ± 0.45 static vs. 0.97 ± 0.25 dynamic), and COL3 expression was elevated for both cases (1.6 ± 0.67 static vs. 1.3 ± 0.41 dynamic). BGL and P4H content was similar between the three sample groups, while expression of MMP1, MMP9, LOX, and HSP47 was closer to baseline in dynamic samples (normalized expressions of 1.07, 1.06, 0.96, and 1.11 respectively) when compared to static samples, in which expression levels were consistently reduced (0.63, 0.69, 0.8, and 0.76). In general, use of dynamic mechanical stimulation appeared to cluster normalized component expression around 1.0 (Figure 11B). Exceptions were VC (static 0.8 ± 0.31 , dynamic 0.70 ± 0.25), COL3 (static 1.59 ± 0.68 , dynamic 1.32 ± 0.41), MMP2 (static 0.58 ± 0.39 , dynamic 2.6 ± 0.89), and MMP13 (static 1.33 ± 0.52 , dynamic 2.6 ± 1.6).

In normal valve tissue, the atrialis is mostly comprised of elastin. Although immunostaining for elastin was not performed, Movat images (Figure 9) show that the elastin layer is maintained after two weeks of dynamic culture. While normalized COL1 expression was reduced in static culture, it was maintained within normal values with dynamic culture (0.75 ± 0.25 static vs. 0.98 ± 0.27 dynamic, $p=0.03$). Although normalized COL3 expression was slightly greater with dynamic culture than static culture (0.88 ± 0.25 static vs. 1.2 ± 0.37 , $p=0.06$), baseline production of this ECM component was maintained in both cases.

Expression of all PGs remained constant compared to baseline with both static and dynamic culture, as did COLL3, MMP1, MMP2, MMP9, and LOX content; this tendency of both treatments to maintain atrialis composition is illustrated in Figure 11C. TIMP1 expression was too varied between samples (0.68 ± 0.32 static vs. 0.74 ± 0.45 dynamic) to draw a conclusion. Dynamic stimulation caused the expression of two factors away from the maintenance range: HSP47 (static 1.32 ± 1.08 , dynamic 0.77 ± 0.26) and MMP13 (static 1.16 ± 0.44 , dynamic 1.6 ± 0.57).

The spongiosa of a healthy mitral valve mostly contains DCN, VC, and BGL. As shown in Figure 11D, dynamic stimulation did not induce a marked overall improvement of component expression over static treatment; selected improvements, however, are highlighted below. Normalized expression of DCN and VC were normal in both the static and dynamic treatments (DCN: 0.92 ± 0.30 static vs. 0.95 ± 0.33 dynamic and VC: 0.91 ± 0.27 static vs. 0.98 ± 0.14 dynamic), while BGL expression was reduced in both culture groups (0.82 ± 0.43 static vs. 0.79 ± 0.28 dynamic). Normalized expression of MMP9 (0.55 ± 0.31 static vs. 1.2 ± 0.72 , $p=0.01$) and TIMP1 (0.79 ± 0.46 vs. 1.3 ± 0.65 , $p=0.04$) in the spongiosa were both greater with dynamic culture and reduced with static culture. MMP2, MMP9, and HSP47 expression was constant between the dynamic culture samples and baseline controls. Their resulting normalized stain intensity, which was approximately 1.0, was greater than and an improvement over that of the static samples. Normalized staining intensity was approximately 1.0 for MMP13, P4H, and LOX in both static and dynamic samples. Dynamic culture caused a reduction in the normalized staining intensity of 3 factors in the spongiosa to outside the maintenance range: COLL1 (static 0.73 ± 0.32 , dynamic 0.71 ± 0.28), MMP2 (static 0.58 ± 0.39 , dynamic 0.53 ± 0.27), and MMP1 (static 1.16 ± 0.61 , dynamic 0.54 ± 0.57).

DISCUSSION

The current study demonstrated that the splashing bioreactor provided mechanical stimulation necessary to preserve normal mitral valve layered structure and ECM composition. In samples cultured without mechanical stimulation, proliferating cells deep within the tissue were depleted, and the layered structure noted in the normal valve became less defined with increased culture time. Fluid movement against tissue surfaces initiated by rotation of the bioreactor chamber provided perfusion and gentle tension, maintaining tissue integrity. This cyclic fluid motion was verified as sufficient to maintain valve structure for the two-week period of interest by assessing stain intensity of PGs, collagen, and ECM turnover mediators before and after culture. This novel bioreactor, though simple in design and construction, could become a powerful tool for both tissue engineering and organ culture applications.

In the pilot study, we found that several major microstructural alterations occur when native heart valve tissue is placed in simple floating organ culture for several weeks. First, there was a dramatic upregulation of collagen and dissipation of PGs and GAGs. An increased abundance of collagen in the longer duration valve organ cultures could be caused by many cellular phenotypic changes, such as the upregulation of collagen producing enzymes and the downregulation of collagen degrading enzymes such as MMPs. A specific phenotypic

analysis of the cells in the valve showed stronger P4H expression corresponding to areas of higher collagen content. We speculated that this apparent collagen upregulation and the rapid disorganization of the collagen layers could be attributed to the absence of mechanical stretch-induced perfusion of the tissues with our organ culture system. The dissipation of PGs could also be caused by the disorganization of the tissue, allowing the water-binding PGs and GAGs to leach out over time.

In addition to ECM changes, cells within the static cultured valves appeared to either migrate or dissipate with time, corroborating earlier static organ culture studies.¹ There were also large buildups of surface cells, especially on the ventricular surface. Over several weeks, the cells gradually became less abundant in the denser fibrosa layer and more abundant in the less dense spongiosa layer. Migration of cells within the organ cultured tissue blocks may have been a means to compensate for deficiencies in diffusive nutrient transport. In normal adult heart valves, cells throughout the leaflets are nourished by diffusion of oxygen and nutrients as opposed to a vascular supply.⁴ Normal diffusion, however, is likely facilitated through the cyclic-stretch-induced perfusion of the tissues, which was not present in the static organ culture system.

A splashing bioreactor was therefore designed with the goal of perfusing and applying gentle stretch to a valve organ culture. Prior to using the bioreactor as a system for *in vitro* testing of valvular disease mechanisms, however, the cyclic mechanical stimulation provided by the fluid motion had to be verified as sufficient for maintaining both the layered valve structure and cell viability. The shear stress and velocity profile of flow was determined computationally, and the observed shear stress was 0.017 Pa. Furthermore, the velocity profile showed turbulence around the free edge of the leaflet. Functional evaluation of the biomechanical signals provided by this system was evident from the maintenance of tissue structure. This was illustrated by overall maintenance in elastin, PG, and collagen expression shown by immunohistostaining and histology (Movat) in dynamically cultured tissue. The lack of change in staining intensity of the ECM turnover mediators also indicated limited turnover of the extracellular matrix during the culture time. Proliferating cells were found throughout both the fresh and dynamically cultured tissue, indicating that the bioreactor was also successful in maintaining cell viability within the valve layers. These results showed that the mechanical stimulation provided by the splashing bioreactor was sufficient to maintain the valve layered structure and cell viability characteristics that were lost with static organ culture methods.

Valve cultured under static conditions tended to display excessive collagen production, and a successful bioreactor would maintain normal collagen composition. P4H has a role in the early non-helical phase of collagen synthesis,³⁴ BGL assists in regulation of fibril diameter,¹⁰ and LOX catalyses the cross-links in the collagen fibers.²³ Increased normalized expression of these three components indicated additional collagen remodeling within the chordae with mechanical stimulation. Overall collagen content in the chordae, however, did not change; dynamic culture expression of COLL1 and COLL3 was almost equivalent to baseline in this highly collagenous tissue. Regulation of collagen remodeling was also noted within the valve leaflet. Considering the general increases in normalized expression of MMP13 (which degrades collagen) as well as COLL1 and COLL3, these data suggest that

mechanical stimulation upregulated collagen production in the atrialis, maintaining collagen content via the appropriate turnover mediators. The increase in normalized COLL3 expression, which is also upregulated in myxomatous valves,³ lends particular weight to this remodeling interpretation. It is also interesting to note that although MMP13 is responsible for cleaving COLL1,^{27, 41} there was no significant decrease in COLL1 staining intensity corresponding to increased MMP13 staining intensity in the fibrosa; this result suggests that after two weeks there was only limited collagen remodeling in the fibrosa of dynamic culture samples. Since MMP13 is associated with collagen turnover,⁴¹ this may have been an attempt to limit the excess collagen deposition noted in the earlier study. TIMP1 is an inhibitor of most MMPs;^{27, 41} its decrease in the fibrosa was possibly responsible for the increase in MMP expression.

Although the mechanical stimulation appeared to alter PG and collagen expression in the rest of the mitral valve, normalized BGL, COLL1, and COLL3 remained lower than normal in the spongiosa in both the static and dynamic culture conditions. Lack of dynamic culture based improvement in BGL and collagen content in the spongiosa was potentially due to the lack of coaptation in the leaflet free edge; while the bioreactor supplied mechanical stimulation from fluid flow, the tissue did not make contact with the opposing posterior leaflet as occurs *in vivo*. Elevated TIMP1 expression suggested that remodeling of the tissue might transpire given a longer culture time.

There were some apparent discrepancies between the collagen results in the two static culture studies (the pilot study and the static culture controls for the bioreactor validation study). The mitral valve tissue cultured statically in the bioreactor validation study demonstrated less staining for COLL1 (the most abundant collagen in normal valves) than baseline after two weeks of static culture, whereas the tissue from the pilot study showed more total collagen with increased culture time, as evidenced by the Movat safran yellow-stained regions (Figure 6). One possible explanation is that the pilot study employed tricuspid valve tissue; the two valves may have had different responses to the culture environment. The greater accumulation of collagen in the pilot study could also be attributed to the longer culture time (up to 8 weeks). In addition, the Movat stain used in the pilot study could not be used to distinguish between the different collagen types present in the valve. In the validation study, both COLL1 and COLL3 were measured via immunostaining, and results suggested that an increase in collagen may have been due to COLL3 upregulation. COLL3 has been shown previously to be greater than normal in patients with myxomatous³ and rheumatic²² heart valve disease and has been presumed to indicate valve pathological remodeling; the increase in COLL3 noted in the current study suggests an ongoing repair process within the tissue.

The exact role of the mechanical stimulation provided by the splashing bioreactor in maintaining ECM components and precursors should be explored in a future study. It is possible that the fluid motion directly impacted mechanical signaling in the tissue. The role of the fluid motion could be further clarified by providing mechanical stimulation in another manner, such as mounting the valve tissue in tension instead of the relaxed state used above, or by employing a different speed of rotation or a different rotation pattern (i.e., rocking vs. continuous). Another possibility is that the splashing of the culture media indirectly

improved nutrient diffusion, which should be assessed in future work by comparing glucose, L-glutamine, ammonia, and lactate content in cell culture medium throughout the culture period. It is also highly likely that the rotating movement of the bioreactor improves transport of oxygen across the gas/fluid interface, thereby increasing the levels of dissolved oxygen in the medium. This improvement in oxygen levels would be beneficial to the valve as it would prevent hypoxia, which can occur when dissolved oxygen levels fall below 20%.³⁸ Therefore, in the future it will be important to compare the dissolved oxygen content in the culture media between static and dynamic culture conditions.

This bioreactor design validation study was novel compared to those used to validate previous heart valve tissue engineering bioreactor designs,³⁹ using a longer time course for the study as well as qualitative and quantitative tissue analysis methods. Previous heart valve bioreactor studies have often focused on demonstrating upregulation of ECM components or precursors after 48 hours.^{15, 28, 39} Conversely, the current study employed a longer culture time, which is more useful for modeling a long-term pathology or for examining the effects of an extended tissue culture period. Furthermore, most heart valve tissue engineering bioreactor studies have used biochemical methods or qualitative immunohistochemical and histological analysis of the overall valve to assess ECM modeling.^{26, 42} The current research is one of few bioreactor studies^{15, 28} that focused on changes of specific ECM components and synthesis mediators within the individual layers, which is important due to their different structure and function. While the results from this current study cannot be directly compared to those of the previous bioreactor studies, when the results are combined, a more complete picture of valvular remodeling can be drawn.

Limitations of this project include the subjectivity of the semi-quantitative immunohistochemical analysis. To eliminate potential bias, all samples were blinded prior to analysis. Repeatability was assessed by a second analysis of the tissues. This method has been previously documented to have a variability of <15%,¹¹ and the current study had a similar level of precision. It is also possible that cell migration noted in the static culture studies was due to a wound response during the initial sample preparation as opposed to nutrient access.²⁰ To mitigate the effect of this preparation artifact on the data, samples sectioned for staining were located deep within the tissue, away from the original cut. Another limitation was that the tissue was only examined at the study endpoint. In the future, an increased study duration with multiple timepoints could track the activity and consequences of ECM turnover mediators that were not preserved, such as MMP2 in the fibrosa. The ECM itself may remodel due to the effects of these mediators.

CONCLUSION

The development and validation of organ culture systems makes available powerful tools to study physiological systems and pathological mechanisms *in vitro* that would otherwise be nearly impossible to observe. This work describes the design of a novel bioreactor with a splashing motion that is intended to cause light stretch and perfusion of the mitral valve tissue to maintain tissue structure. Validation is an important step; maintenance of both ECM structure and cell concentration within the different layers of the tissue indicated successful organ culture when the bioreactor was used, while valve tissue cultured without

mechanical stimulation displayed loss of the layered structure, cell loss deep within the tissue, altered collagen content, and reduced PG content. With this successful design, this bioreactor can be used to study the early mechanisms of valvular heart disease. Alternately, the design could be modified for use towards the tissue engineering of heart valves with the introduction of a treated scaffold material and donor cells². The size of the entire system could also be scaled up to accommodate an entire valve, which would more faithfully reproduce the coaptation of the leaflet free edges. In the future, this straightforward system can be used in a myriad of applications to promote further investigation of heart valve biology, pathology, and therapies.

Acknowledgments

The authors acknowledge funding from the National Science Foundation (grant #0502342). J.E.B. was supported by an NSF graduate research supplement. A.E.C. was supported by an NSF REU supplement. A.S.M. was supported by an institutional NSF REU program at the Cleveland Clinic Foundation.

ABBREVIATIONS

BGL	Biglycan
COLL	Collagen
DCN	Decorin
ECM	Extracellular Matrix
GAG	Glycosaminoglycan
HSP47	Heat Shock Protein 47
LOX	Lysyl Oxidase
MMP	Matrix Metalloproteinase
P4H	Prolyl-4-Hydroxylase
PCNA	Proliferating Cell Nuclear Antigen
PG	Proteoglycan
TIMP	Tissue Inhibitor of Matrix Metalloproteinase
VC	Versican

References

1. Allison DD, Drazba JA, Vesely I, Kader KN, Grande-Allen KJ. Cell viability mapping within long-term heart valve organ cultures. *J Heart Valve Dis.* 2004; 13:290–6. [PubMed: 15086269]
2. Barzilla JE, Blevins TL, Grande-Allen KJ. Age-related structural changes in cardiac valves: implications for tissue-engineered repairs. *Am J Geriatr Cardiol.* 2006; 15:311–5. [PubMed: 16957451]
3. Cole WG, Chan D, Hickey AJ, Wilcken DE. Collagen composition of normal and myxomatous human mitral heart valves. *Biochem J.* 1984; 219:451–60. [PubMed: 6430269]
4. Duran CM, Gunning AJ. The vascularization of the heart valves: a comparative study. *Cardiovasc Res.* 1968; 2:290–6. [PubMed: 5670736]

5. Engelmayr GC Jr, Hildebrand DK, Sutherland FW, Mayer JE Jr, Sacks MS. A novel bioreactor for the dynamic flexural stimulation of tissue engineered heart valve biomaterials. *Biomaterials*. 2003; 24:2523–32. [PubMed: 12695079]
6. Engelmayr GC Jr, Rabkin E, Sutherland FW, Schoen FJ, Mayer JE Jr, Sacks MS. The independent role of cyclic flexure in the early in vitro development of an engineered heart valve tissue. *Biomaterials*. 2005; 26:175–87. [PubMed: 15207464]
7. Engelmayr GC Jr, Sales VL, Mayer JE Jr, Sacks MS. Cyclic flexure and laminar flow synergistically accelerate mesenchymal stem cell-mediated engineered tissue formation: Implications for engineered heart valve tissues. *Biomaterials*. 2006; 27:6083–95. [PubMed: 16930686]
8. Engelmayr GC Jr, Soletti L, Vigmostad SC, Budilarto SG, Federspiel WJ, Chandran KB, Vorp DA, Sacks MS. A novel flex-stretch-flow bioreactor for the study of engineered heart valve tissue mechanobiology. *Ann Biomed Eng*. 2008; 36:700–12. [PubMed: 18253834]
9. Fisher LW, Termine JD, Young MF. Deduced protein sequence of bone small proteoglycan I (biglycan) shows homology with proteoglycan II (decorin) and several nonconnective tissue proteins in a variety of species. *J Biol Chem*. 1989; 264:4571–6. [PubMed: 2647739]
10. Grande-Allen KJ, Calabro A, Gupta V, Wight TN, Hascall VC, Vesely I. Glycosaminoglycans and proteoglycans in normal mitral valve leaflets and chordae: association with regions of tensile and compressive loading. *Glycobiology*. 2004; 14:621–33. [PubMed: 15044391]
11. Gupta V, Barzilla JE, Mendez JS, Stephens EH, Lee EL, Collard CD, Laucirica R, Weigel PH, Grande-Allen KJ. Abundance and location of proteoglycans and hyaluronan within normal and myxomatous mitral valves. *Cardiovasc Pathol*. 2009; 18:191–197. [PubMed: 18621549]
12. Hildebrand DK, Wu ZJ, Mayer JE Jr, Sacks MS. Design and hydrodynamic evaluation of a novel pulsatile bioreactor for biologically active heart valves. *Ann Biomed Eng*. 2004; 32:1039–49. [PubMed: 15446500]
13. Hunt S, Spitznas M, Seifert P, Rauwolf M. Organ culture of human main and accessory lacrimal glands and their secretory behaviour. *Exp Eye Res*. 1996; 62:541–54. [PubMed: 8759522]
14. Jaffer FA, Nahrendorf M, Sosnovik D, Kelly KA, Aikawa E, Weissleder R. Cellular imaging of inflammation in atherosclerosis using magnetofluorescent nanomaterials. *Mol Imaging*. 2006; 5:85–92. [PubMed: 16954022]
15. Konduri S, Xing Y, Warnock JN, He Z, Yoganathan AP. Normal physiological conditions maintain the biological characteristics of porcine aortic heart valves: an ex vivo organ culture study. *Ann Biomed Eng*. 2005; 33:1158–66. [PubMed: 16133923]
16. Krishnamurthy G, Ennis DB, Itoh A, Bothe W, Swanson JC, Karlsson M, Kuhl E, Miller DC, Ingels NB Jr. Material properties of the ovine mitral valve anterior leaflet in vivo from inverse finite element analysis. *Am J Physiol Heart Circ Physiol*. 2008; 295:H1141–H1149. [PubMed: 18621858]
17. Kunzelman KS, Cochran RP. Stress/strain characteristics of porcine mitral valve tissue: parallel versus perpendicular collagen orientation. *J Card Surg*. 1992; 7:71–8. [PubMed: 1554980]
18. Kunzelman KS, Cochran RP, Verrier ED, Eberhart RC. Anatomic basis for mitral valve modelling. *J Heart Valve Dis*. 1994; 3:491–6. [PubMed: 8000582]
19. Lester WM, Damji AA, Gedeon I, Tanaka M. Interstitial cells from the atrial and ventricular sides of the bovine mitral valve respond differently to denuding endocardial injury. *In Vitro Cell Dev Biol*. 1993; 29A:41–50. [PubMed: 8095255]
20. Lester WM, Damji AA, Tanaka M, Gedeon I. Bovine mitral valve organ culture: role of interstitial cells in repair of valvular injury. *J Mol Cell Cardiol*. 1992; 24:43–53. [PubMed: 1532992]
21. Lester WM, Gotlieb AI. In vitro repair of the wounded porcine mitral valve. *Circ Res*. 1988; 62:833–45. [PubMed: 3127074]
22. Lis Y, Burleigh MC, Parker DJ, Child AH, Hogg J, Davies MJ. Biochemical characterization of individual normal, floppy and rheumatic human mitral valves. *Biochem J*. 1987; 244:597–603. [PubMed: 3446179]
23. Maki JM, Sormunen R, Lippo S, Kaartenaho-Wiik R, Soininen R, Myllyharju J. Lysyl oxidase is essential for normal development and function of the respiratory system and for the integrity of

- elastic and collagen fibers in various tissues. *Am J Pathol.* 2005; 167:927–36. [PubMed: 16192629]
24. Menter, FR. Zonal two equation $k-\omega$ turbulence models for aerodynamic flows. 24th AIAA Fluid Dynamics Conference; 1993; Orlando, FL. 1993. AIAA Paper 93–2906
 25. Merrick AF, Shewring LD, Cunningham SA, Gustafsson K, Fabre JW. Organ culture of arteries for experimental studies of vascular endothelium in situ. *Transpl Immunol.* 1997; 5:3–9. [PubMed: 9106328]
 26. Merryman WD, Lukoff HD, Long RA, Engelmayr GC Jr, Hopkins RA, Sacks MS. Synergistic effects of cyclic tension and transforming growth factor-beta1 on the aortic valve myofibroblast. *Cardiovasc Pathol.* 2007; 16:268–76. [PubMed: 17868877]
 27. Nagase H, Visse R, Murphy G. Structure and function of matrix metalloproteinases and TIMPs. *Cardiovasc Res.* 2006; 69:562–73. [PubMed: 16405877]
 28. Platt MO, Xing Y, Jo H, Yoganathan AP. Cyclic pressure and shear stress regulate matrix metalloproteinases and cathepsin activity in porcine aortic valves. *J Heart Valve Dis.* 2006; 15:622–9. [PubMed: 17044366]
 29. Prior R, D'Urso D, Frank R, Prikulis I, Wihl G, Pavlakovic G. Canine leptomenigeal organ culture: a new experimental model for cerebrovascular beta-amyloidosis. *J Neurosci Methods.* 1996; 68:143–8. [PubMed: 8912187]
 30. Sacks MS, Enomoto Y, Graybill JR, Merryman WD, Zeeshan A, Yoganathan AP, Levy RJ, Gorman RC, Gorman JH 3rd. In-vivo dynamic deformation of the mitral valve anterior leaflet. *Ann Thorac Surg.* 2006; 82:1369–77. [PubMed: 16996935]
 31. Sadgrove MP, Chad JE, Gray WP. Kainic acid induces rapid cell death followed by transiently reduced cell proliferation in the immature granule cell layer of rat organotypic hippocampal slice cultures. *Brain Res.* 2005; 1035:111–9. [PubMed: 15722051]
 32. Sands MP, Rittenhouse EA, Mohri H, Merendino KA. An anatomical comparison of human pig, calf, and sheep aortic valves. *Ann Thorac Surg.* 1969; 8:407–14. [PubMed: 5353458]
 33. Stephens EH, de Jonge N, McNeill MP, Durst CA, Grande-Allen KJ. Age-related changes in material behavior of porcine mitral and aortic valves and correlation to matrix composition. *Tissue Eng Part A.* 2010; 16:867–78. [PubMed: 19814589]
 34. Tasab M, Batten MR, Bulleid NJ. Hsp47: a molecular chaperone that interacts with and stabilizes correctly-folded procollagen. *Embo J.* 2000; 19:2204–11. [PubMed: 10811611]
 35. Taylor PM, Allen SP, Yacoub MH. Phenotypic and functional characterization of interstitial cells from human heart valves, pericardium and skin. *J Heart Valve Dis.* 2000; 9:150–8. [PubMed: 10678389]
 36. Veranic P, Psenicnik M. A mini organ culture as a model for studying the gallbladder epithelium of mouse. *Biol Cell.* 1996; 88:145–51. [PubMed: 9237371]
 37. Walker GA, Masters KS, Shah DN, Anseth KS, Leinwand LA. Valvular myofibroblast activation by transforming growth factor-beta: implications for pathological extracellular matrix remodeling in heart valve disease. *Circ Res.* 2004; 95:253–60. [PubMed: 15217906]
 38. Warnock JN, Konduri S, He Z, Yoganathan AP. Design of a sterile organ culture system for the ex vivo study of aortic heart valves. *J Biomech Eng.* 2005; 127:857–61. [PubMed: 16248316]
 39. Weston MW, Yoganathan AP. Biosynthetic activity in heart valve leaflets in response to in vitro flow environments. *Ann Biomed Eng.* 2001; 29:752–63. [PubMed: 11599583]
 40. Wiester LM, Giachelli CM. Expression and function of the integrin alpha9beta1 in bovine aortic valve interstitial cells. *J Heart Valve Dis.* 2003; 12:605–16. [PubMed: 14565714]
 41. Woessner, JF.; Nagase, H. *Matrix Metalloproteinases and TIMPs.* New York: Oxford University Press; 2000. p. 223
 42. Xing Y, Warnock JN, He Z, Hilbert SL, Yoganathan AP. Cyclic pressure affects the biological properties of porcine aortic valve leaflets in a magnitude and frequency dependent manner. *Ann Biomed Eng.* 2004; 32:1461–70. [PubMed: 15636107]

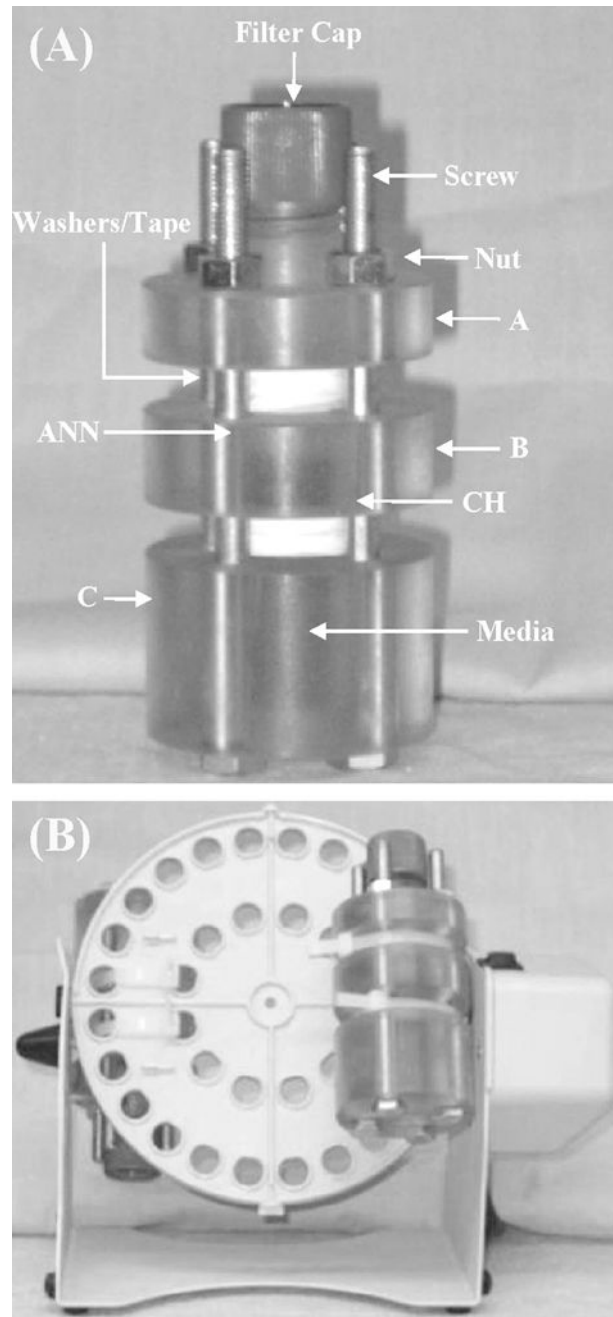


Figure 1.

A. Splashing bioreactor chamber. The chamber is comprised of three hollow segments (A, B, and C) into which the valve segment is mounted. The media inside the chamber provides nutrients to the tissue. Valve attachment sites (inside chamber) are also indicated.

ANN=annulus, CH=chordae. B: Bioreactor on rotator. The pallet rotates 360 degrees, forcing media over the valve surfaces.

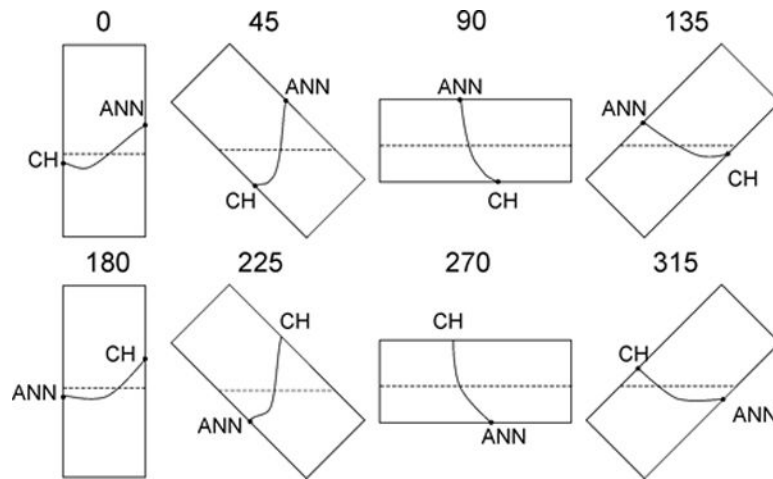


Figure 2. Rotation of splashing bioreactor through 360° motion. As the chamber rotates, the culture medium flows past the tissue surface, imparting normal and shear forces to the surface and causing deformation of the organ culture.

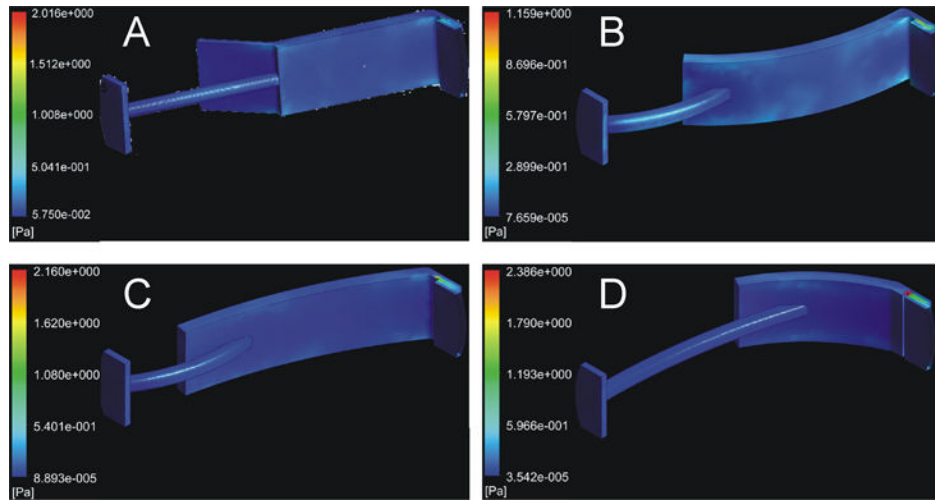


Figure 3. Plot of shear stress on the surface of the leaflet. Shear stress was averaged over the shown surface of the leaflet. (A) Shear stress at system orientation 0° (straight up and down). (B) Shear stress at system orientation 45° , (C) shear stress at system orientation 90° (horizontal), (D) shear stress at system orientation 135° .

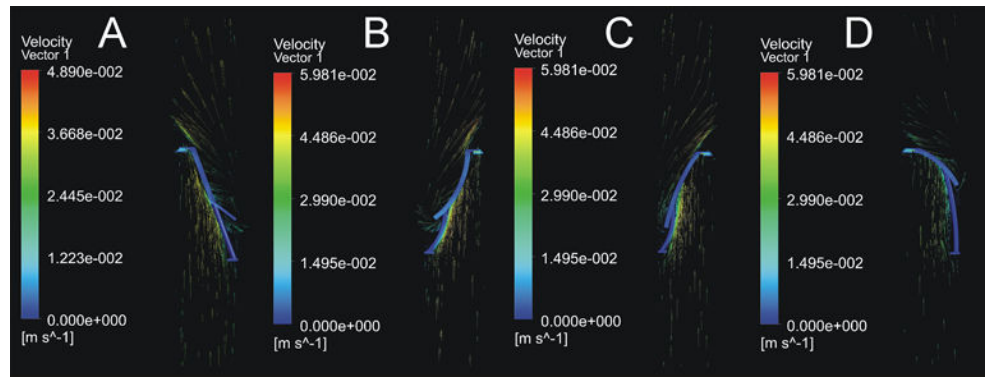


Figure 4.

Vector plot of fluid velocity in the mid-plane of the culture chamber. Fluid velocity peaks at ~ 4 cm/s near the area of chordal attachment to the leaflet. Eddies can be observed near the free edge. (A) Velocity vectors at system orientation 0° , (B) velocity vectors at system orientation 45° , (C) velocity vectors at system orientation 90° , (D) velocity vectors at system orientation 135° .

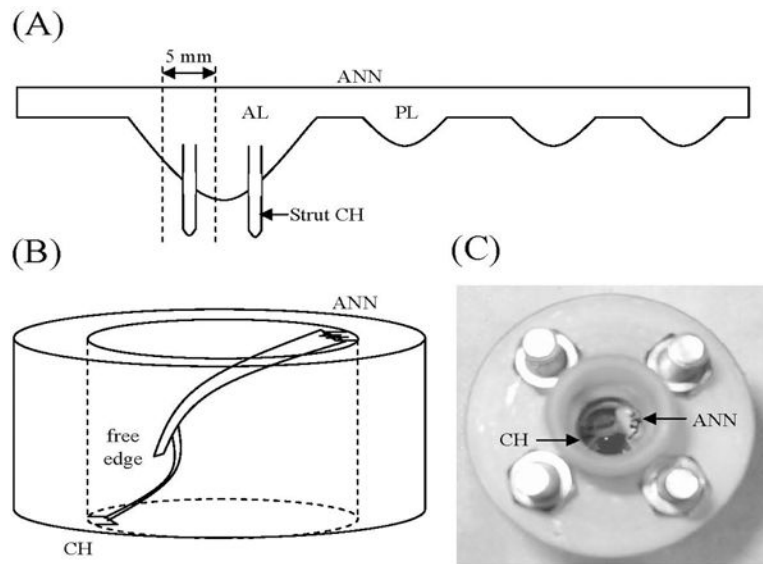


Figure 5. Valve insertion. (A) A 5 mm radial valve segment is removed from the AL. (B) The segment is then mounted at the ANN and CH, taking care to leave the tissue slack. The free edge is unattached. (C) Top view of valve in bioreactor. AL=anterior leaflet, ANN=annulus, CH=chordae, PL=posterior leaflet.

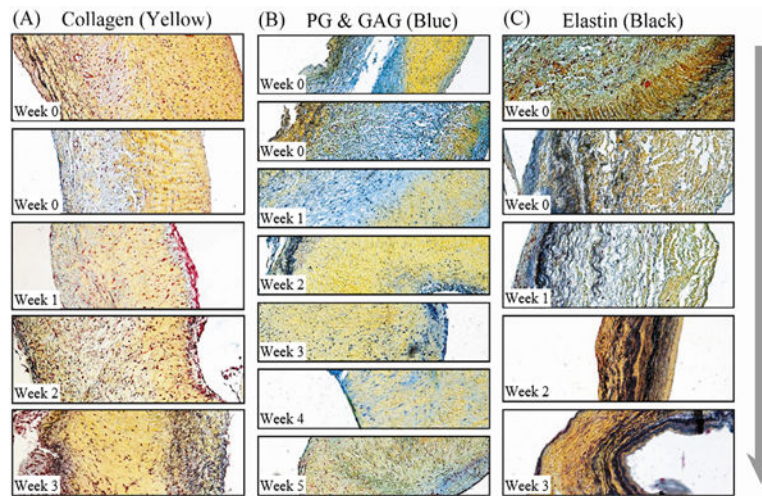


Figure 6. Movat pentachrome stained sections of porcine organ cultured valve tissue blocks (original magnification 10X). The ventricular surfaces are on the right and the atrial surfaces are on the left. (a) Collagen content (yellow) clearly dispersed from the normal structure and began to dominate the valves, usually becoming the only remaining matrix protein by the conclusion of culture. (b) PG and GAG content (blue-green) gradually disappeared, becoming just a diffuse haze in the mixture. (c) Elastin (black) became less localized and occasionally dominated the cross section, often together with collagen. Arrow indicates increase in culture duration.

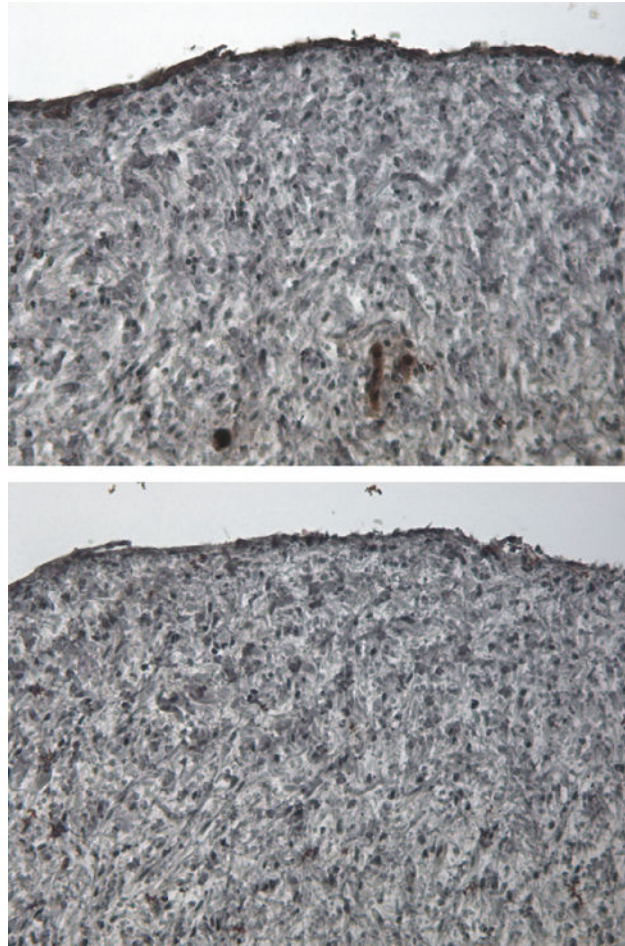


Figure 7. Valve section stained with von Willebrand Factor (vWF, top) and the corresponding negative stain (bottom) of fresh tissue immediately after sectioning into culture segments. Dark brown stain along the surfaces in the vWF section indicated the presence of an intact endothelial layer prior to organ culture.

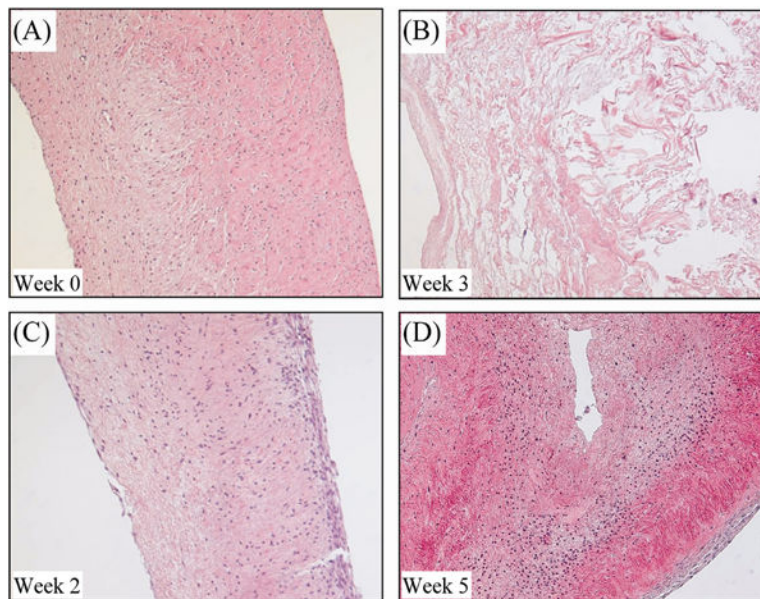


Figure 8. Hematoxylin and eosin stained sections of porcine organ cultured valve tissue blocks (original magnification 10X). The ventricular surfaces are on the right and the atrial surfaces are on the left. When compared to the control (A), valve tissue cultured without mechanical stimulation experienced (B) cell depletion pattern, (C) cell accumulation on the ventricular surface, and (D) cell clumping/migration from more dense tissue to less dense, more hydrated tissue.

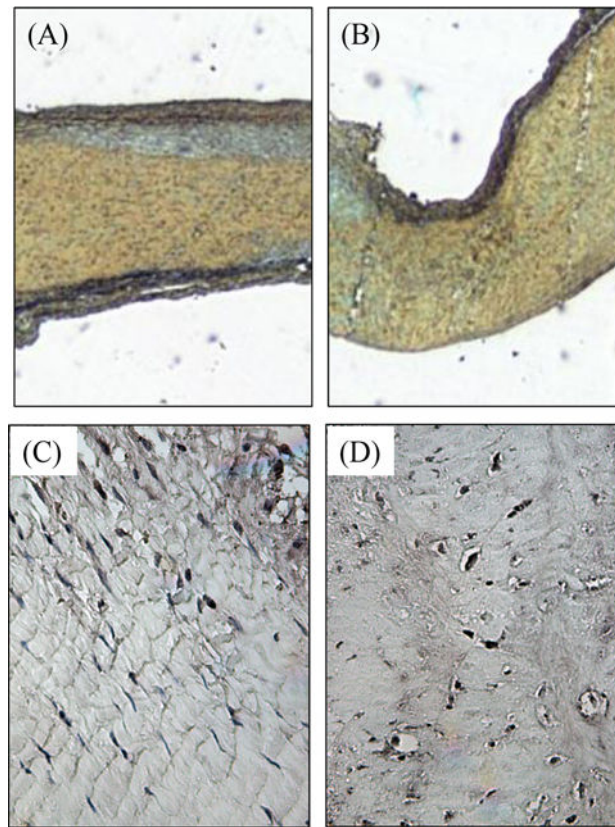


Figure 9. Comparison of a mitral valve center before (A, C) and after (B, D) two weeks of dynamic organ culture. When compared to the uncultured fresh control (A), Movat staining shows a maintenance of atrialis (top black) and fibrosa (yellow) layers after two weeks of culture (B). PCNA stain in the fresh control (C) and the cultured (D) tissues shows the presence of proliferating cells (in brown) throughout the tissue. Atrial surface at top. Magnification = 5X (A, B) or 20X (C, D).

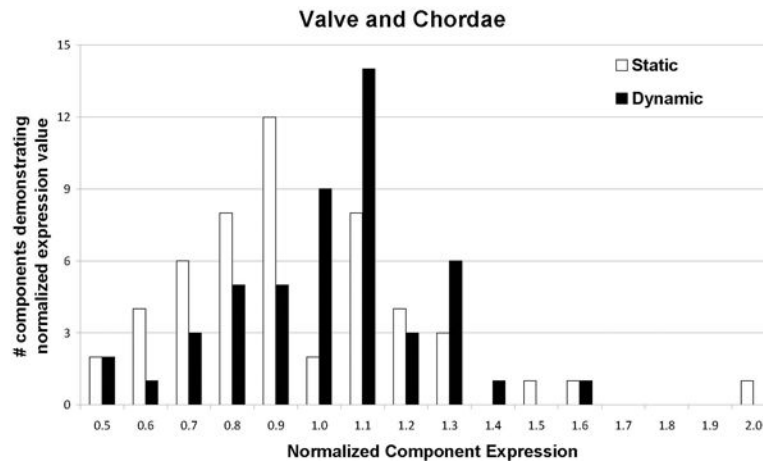


Figure 10.

Histogram showing normalized component expression throughout the mitral valve. To generate the above histogram, the expression levels for all examined components (each of which was normalized to its matched fresh control) for all layers/chordae of the mitral valve samples were categorized into increments of 0.1. Samples cultured under static (white) and dynamic (black) conditions were compared using this histogram to gain a picture of the overall status of extracellular matrix within the cultured valves. In general, dynamic culture conditions contributed to component maintenance as defined by 1.0 ± 0.2 ($100 \pm 20\%$), after two weeks of culture. Not shown: normalized expression of MMP13 (2.3) and MMP2 (2.6) in fibrosa of dynamically cultured valves.

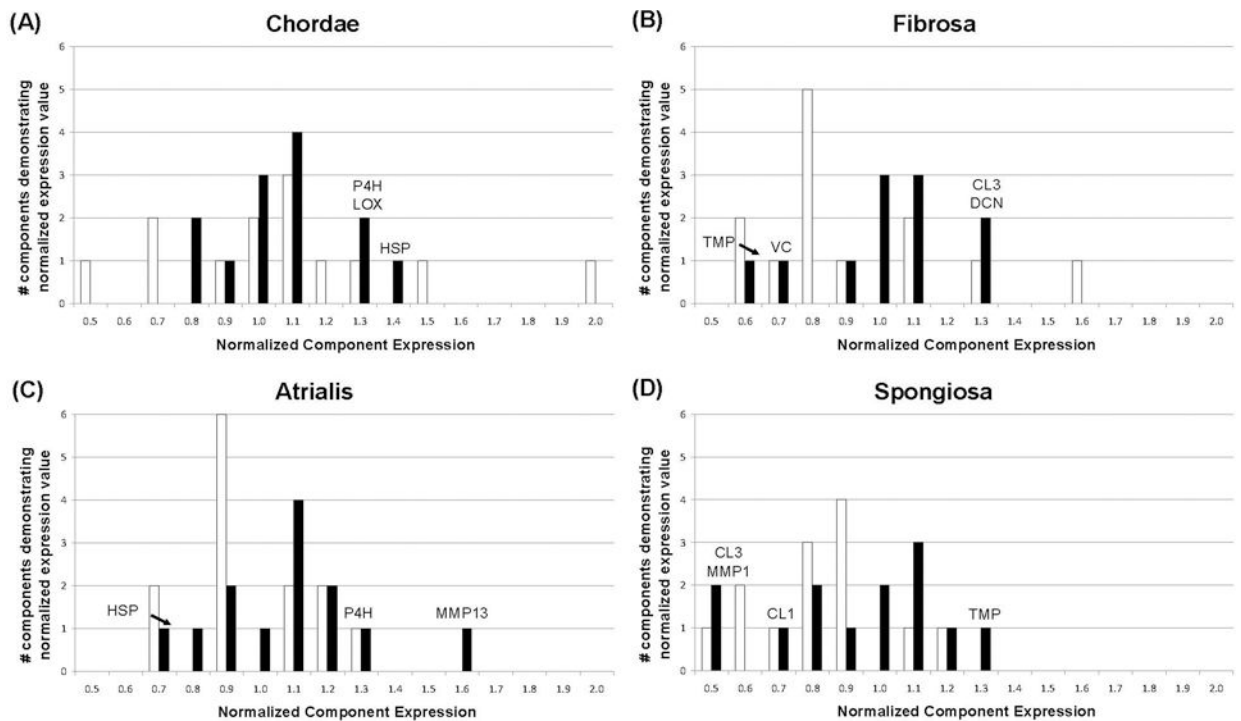


Figure 11.

Histogram showing normalized component expression in the mitral valve chordae (A), fibrosa (B), atrialis (C), and spongiosa (D) to permit comparison of the samples cultured under static (white) and dynamic (black) conditions. These histograms were generated in the same manner as that described in the legend to Figure 10. In general, dynamic culture conditions contributed to component maintenance as defined by 1.0 ± 0.2 ($100 \pm 20\%$) after 2 weeks of culture; the components considered to be maintained are described in the text and shown in Table 1 by the “-“ symbol. ECM components and synthesis/turnover mediators not maintained by dynamic culture are indicated above bars, and are also indicated in Table 1 by the up or down arrows. Not shown: normalized expression of MMP13 (2.3) and MMP2 (2.6) in fibrosa of dynamically cultured valves. Abbreviations are as given in text except for HSP = heat shock protein 47, CL1 = collagen type 1, CL3 = collagen type 3, TMP = tissue inhibitor of metalloproteases.

Table 1

Change in abundance of ECM component/precursor after culture

	AT	SP	FB	CH
BGL	-/-	-/-	-/-	-/↑
DCN	-/-	-/-	-/↑	-/-
VC	-/-	-/-	-/↓	↓/-
COLL1	↓/-	↓/↓	-/-	↓/-
COLL3	-/-	↓/↓	↑/↑	↑/-
P4H	-/↑	-/-	-/-	-/↑
MMP1	-/-	-/↓	↓/-	-/-
MMP2	-/-	-/-	↓/↑	-/-
MMP9	-/-	↓/-	↓/-	↑/-
MMP13	-/↑	-/-	↑/↑	-/-
TIMP1	↓/↓	-/↑	-/↓	-/-
LOX	-/-	-/-	-/-	↓/↑
HSP47	↑/-	↓/-	-/-	↑/-

Symbols before or after slash mark indicate changes in specified component after two weeks of static/dynamic culture relative to fresh tissue.

AT: Atrialis; SP: spongiosa; FB: fibrosa; CH: chordae.

–: No change in normalized content expression (1.0 ± 0.2).

↑: Increase in normalized content expression.

↓: Decrease in normalized content expression.